Available online at www.sciencedirect.com
ScienceDirect
Journal of Nuclear Materials 356 (2006) 95–104
journal of nuclear materials
www.elsevier.com/locate/jnucmat

Effect of gas atoms and displacement damage on mechanical properties and microstructures of F82H

E. Wakai [a,*], M. Ando [a], T. Sawai [a], K. Kikuchi [a], K. Furuya [b], M. Sato [a], K. Oka [c], S. Ohnuki [c], H. Tomita [a], T. Tomita [a], Y. Kato [a], F. Takada [a]

[a] *Japan Atomic Energy Agency, Nuclear Science and Engineering Directorate, Research Group for Irradiation Field Materials, Tokai-mura, Ibaraki-ken 319-1195, Japan*
[b] *National College of Technology, Hachinohe, Aomori-ken 039-1192, Japan*
[c] *Hokkaido University, Kita-ku, Sapporo 060-8628, Japan*

Abstract

Effects of displacement damage and gas atoms on microstructures and mechanical properties of F82H steel were examined by some various different methods. The hardness of F82H was increased by triple beams, dual beams and single beam at 270 °C to 20 dpa and 360 °C to 50 dpa, and the increment of hardness by irradiation at 360 °C was larger than that at 270 °C. The increment of hardness due to triple, dual and single beams depended on the irradiation temperatures. The peak temperature of swelling induced by dual ion beams to 50 dpa was about 430 °C at temperatures from 360 to 600 °C and the value of swelling was about 0.6%. Strength of F82H-std steel tested at 600 and 700 °C by small punch (SP) was increased by about 84 appm helium implantation at 120 °C, and no degradation in ductility was observed. In a 0.18DCT fracture toughness test performed at 300 °C of ductile properties, the strength of F82H with helium production was rapidly decreased as compared to that with no helium production beyond a maximum strength in ductile temperature region. The cause is related to the occurrence of sub-boundary, such as lath boundaries and packed boundaries, cracking due to helium migration to sub-boundaries. From these results, the design window of safety zone of F82H steel for operation of nuclear environment systems may be modified.

1. Introduction

Ferritic/martensitic steels are one of the candidate materials for the vessel of the spallation target [1], and reduced-activation ferritic/martensitic (RAF) steels are first priority materials of structure for fusion nuclear reactors [2]. In these systems, particles with high energy irradiate the vessels or structures, and helium and hydrogen atoms are generated in materials. These systems are desired to operate at relatively higher temperatures. It is reported that helium atoms can affect DBTT [3–7], swelling behavior [8–15] and irradiation hardening [16–23] in martensitic steels.

* Corresponding author. Tel.: +81 29 282 6563; fax: +81 29 282 5922.
E-mail address: wakai.eiichi@jaea.go.jp (E. Wakai).

0022-3115/$ - see front matter © 2006 Elsevier B.V. All rights reserved.
doi:10.1016/j.jnucmat.2006.05.032

To study the synergistic effects of displacement damage and helium on mechanical properties and microstructure, there are some specific experimental methods. The synergistic effect can be examined by using high energy proton beams to irradiate target materials such as SINQ (Swiss Spallation Neutron Source) [24] and LANSCE (Los Alamos Neutron Science Center) [25]. Reactor neutron irradiation with helium production can be partially simulated by martensitic steels doped with ^{10}B or ^{58}Ni in a mixed spectrum fission reactor [12,26–28]. A multi-ion irradiation experiment is also a very important method to control the helium production ratio during irradiation [8,9,11,17]. Particularly, this method produces fusion relevant high-energy cascades at controllable helium production (He/dpa). Moreover, the effects of helium on radiation hardening behavior can be evaluated by combining ion-irradiation experiments and an ultra microindentation technique [16,17]. The effects of helium atoms on mechanical properties and microstructures can also be examined by the cyclotron helium implantation [3,29–33], and hardness changes, DBTT shift, fracture behaviors and creep strength [30,31] of martensitic steels due to helium have been investigated after irradiation.

In this study, the dependence of irradiation temperature and gas atoms on swelling, irradiation hardening and DBTT shift in martensitic F82H steel have been examined by some experimental methods such as multiple ion beams, cyclotron helium implantation and neutron irradiation of boron-doped steels.

2. Experimental procedure

2.1. Multiple ion beam experiments of hardness and microstructures

The chemical compositions of F82H-std steels used in this study are given in Table 1. The heat treatment of F82H steel consisted of first normalizing at 1040 °C for 38 min and tempering at 750 °C for 1 h. The material was cut to small coupon type specimens ($6 \times 2 \times 0.8$ mm^3). One of the 6×0.8 mm sides was irradiated after polishing with SiC paper #4000 and 0.3 μm alumina powder and finally to an electrolytic surface polishing. The ion-beam irradiation experiment was carried out at the TIARA facility in JAERI. The configuration of the beam lines and specimens is shown in Fig. 1. The specimens were irradiated at 270, 360 and 430 °C. Single irradiation was performed with 10.5 MeV-Fe^{3+} ions. Dual irradiation was also performed with simultaneous beams of 10.5 MeV-Fe^{3+} and 1.05 MeV-He^{+} ions using an energy degrader for helium ions. Triple irradiation was done with simultaneous beams of 10.5 MeV-Fe^{3+}, 1.05 MeV-He^{+} and 0.38 MeV-H^{+} ions using energy degraders for helium and hydrogen atoms. Helium and hydrogen implantations were performed using an aluminum foil energy degraders in order to control the helium and hydrogen distributions in the depth range of about 0.8–1.3 μm from the specimen surface. The irradiation was performed to 20–50 dpa at the depth of 1.0 μm from the irradiation surface. The damage rate was about 1.0×10^{-3} dpa/s. The

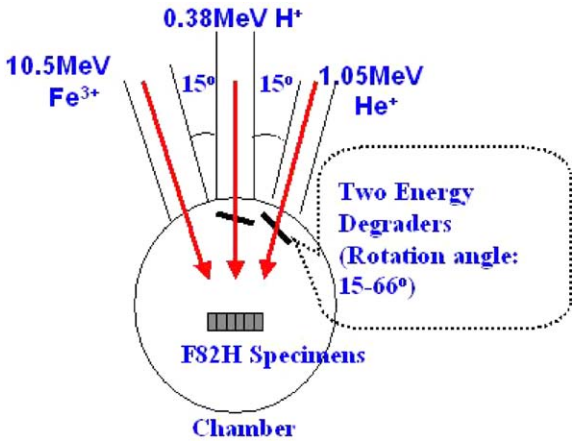

Fig. 1. Schematic configuration of three beam lines, two energy degraders and specimens. The ratios of He/dpa and H/dpa were controlled by degraders.

Table 1
Chemical compositions of F82H-std and F82H doped with ^{10}B, ^{11}B and $^{10}B + ^{11}B$ steels used in this study (wt%)

Materials	B	C	Si	Mn	P	S	Cr	W	V	Ta
F82H	0.0002	0.09	0.07	0.1	0.003	0.001	7.82	1.98	0.19	0.04
F82H + ^{10}B	0.0061	0.097	0.10	0.10	0.007	0.001	7.96	1.98	0.18	0.05
F82H + ^{11}B	0.0059	0.093	0.11	0.10	0.007	0.001	8.02	1.98	0.18	0.05
F82H + ^{10}B + ^{11}B	0.0067	0.094	0.12	0.90	0.007	0.001	8.01	2.01	0.18	0.05

ratios of helium and hydrogen to dpa were about 10 appm He/dpa and 40 appm H/dpa, respectively. The irradiated specimens were then indentation-tested at a load range of 10–25 mN using an UMIS-2000 (CSIRO, Australia) ultra microindentation testing system. The direction of indentation was chosen to be parallel to the ion beam axis or normal to the irradiated surface. The shape of the indenter tip was a Berkovich tip. The nano-microindentation results were analyzed in the manner outlined by Oliver and Pharr [34]. Nano-microindentation tests were performed at loads to penetrate about 0.40 μm in this study as shown in Fig. 2. TEM foils of the ion-irradiated specimens were made by using a Hitachi FB-2000A focused ion beam (FIB) processing instrument with microsampling system operated at 30 kV by Ga^+ ions at the Tokai Hot Laboratory. FIB technique may induce displacement damage on the surface of specimen. In order to remove the damage layer formed by the FIB processing, a low energy Ar ion gun operated at 1 kV and 0.2 kV was applied. The microstructural examination was carried out using a Hitachi-HF-2000 transmission electron microscope (TEM) operated at 200 kV.

2.2. Cyclotron helium implantation experiment and small punch test for 3 mmϕ disk

The TEM disk specimens of F82H-std steel with 0.3 mm thickness were implanted at about 120 °C with a beam of 50 MeV-He^{2+} particles by AVF cyclotron at TIARA facility of JAERI. An energy degrader was used to implant helium into the specimens from top to bottom uniformly [35]. The concentration of the He and displacement damage in the specimen implanted by cyclotron irradiation was evaluated as about 85 appm He and 0.03 dpa, respectively. After the helium implantation experiment, SP experiment and TEM observations were performed. TEM specimen was prepared using a conventional jet-electropolishing. The effect of helium production on fracture behavior at 20, 600 and 700 °C was examined by small punch (SP) tests. The fracture surfaces were observed by a scanning electron microscope (SEM) after the SP. The SP test was graphically shown in Fig. 3.

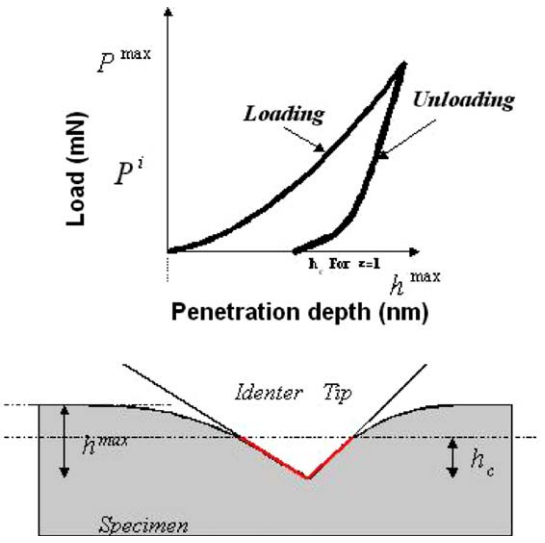

Fig. 2. The direction of indentation was chosen to be parallel to the ion beam axis or normal to the irradiated surface. The shape of the indenter tip was a Berkovich tip.

2.3. Neutron Irradiation of tensile and fracture toughness specimens

The materials used in this study and the compositions are also given in Table 1. In order to produce helium atoms during irradiation the materials were doped with about 60 mass ppm ^{10}B. The purity of isotope elements of ^{10}B and ^{11}B used in this study was about 95%. The plates of these materials with about 15 mm thickness were normalized at 1040 °C for 40 min and tempered at 750 °C for 60 min 0.18DCT and SS-3 specimens were used to evaluate fracture behavior and hardening in this study. The 0.18DCT specimens (12.5 mm diameter and 4.63 mm thickness) were machined in the *T–L* orientation so that crack propagation occurred parallel to the rolling direction. Fatigue pre-cracking was

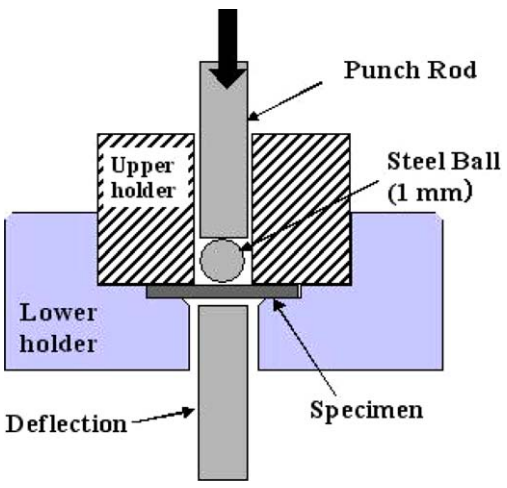

Fig. 3. Small punch testing machine and ϕ3 mm specimen.

performed at room temperature in a condition of crack length to specimen width ratio (a/W) of approximately 0.46. This was followed by side-grooving on each side to depth of ~10% of specimen thickness. The SS-3 tensile specimens were 0.76 mm thick with a gage length of 7.62 mm and 1.55 mm in width. Irradiation was carried out at nominally 300 °C in the capsule 00M-65A of the Japan Materials Test Reactor (JMTR) in the Japan Atomic Energy Agency (JAEA) to neutron fluences of 1.4×10^{21} n/cm^2 ($E>1$ MeV) and 1.2×10^{21} n/cm^2 ($E<0.683$ eV), resulting in a displacement damage of ~2.2 dpa. The averaged displacement damage induced by the reaction of $^{10}B(n,\alpha)^7Li$ was calculated as about 0.2 and 0.1 dpa for the F82H + ^{10}B and F82H + ^{11}B + ^{10}B, respectively. The total displacement damage due to the transmutation reaction and neutron irradiation was 2.4 dpa in the F82H + ^{10}B. After the neutron irradiation, tensile testing was carried out in vacuum at a strain rate of 4×10^{-4} s^{-1} at 25 °C and fracture toughness testing was also performed in a hot cell of the JMTR hot laboratory. After theses tests, the fracture surface was observed by a scanning electron microscope (SEM). The concentrations of helium in the specimens after the irradiations were measured by using a mass analyzer of magnetic reflection type [3]. The helium concentrations produced from a reaction of $^{10}B(n,\alpha)^7Li$ in the F82H + B steels irradiated in the JMTR were evaluated and the helium concentrations produced in the F82H + ^{10}B, F82H + ^{11}B and F82H + ^{10}B + ^{11}B steels were about 330, 14 and 190 appm, respectively.

3. Results and discussion

3.1. Irradiation hardening by ion irradiations

Fig. 4 shows the dose dependence of irradiation hardening at 360 °C up to 50 dpa in F82H martensitic steel. The nano-hardness of F82H steel rapidly increased up to 20 dpa and it tended to saturate from 20 dpa to 50 dpa. The hardness of F82H irradiated with triple beams was slightly higher than the others, and the hardness of F82H irradiated with dual beams was slightly higher than the single irradiation. The difference of hardness of F82H steel irradiated to 50 dpa between single irradiation and multiple irradiations was smaller than that to 20 dpa. The enhancements of hardness due to the multiple irradiations are indicated that the implanted helium and hydrogen atoms in martensitic steel can affect on

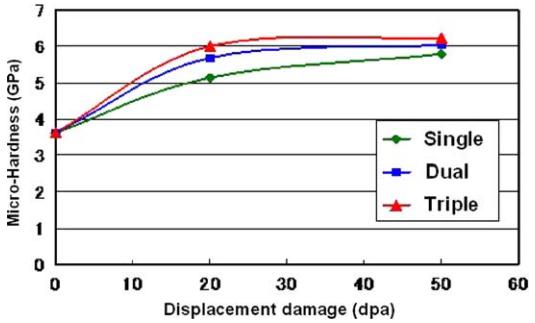

Fig. 4. Changes of hardness of F82H steel irradiated at 360 °C to 50 dpa under single, dual and triple beams in TIARA facility.

irradiation hardening at 360 °C. According to Ando et al. [16], irradiation hardening could be enhanced by the ratio of helium implantation to displacement damage and total amount helium concentration, and the enhancement of hardening was related to the formation of cavities. Similar result for the enhancement of irradiation hardening due to high amounts of helium atoms was reported [19]. Fig. 5 shows the hardness changes of F82H steel irradiated at 270 and 360 °C to 20 dpa under single, dual and triple irradiations. Radiation hardening for single irradiation, dual irradiation and triple irradiation was very similar to each other, and the results were different from those at 360 °C to 20 dpa. Radiation hardening due to single irradiation in F82H steel irradiated at 270 °C was comparable to that due to single irradiation at 360 °C, while the irradiation hardening due to multiple irradiations at 270 °C was smaller than that at 360 °C. The difference of beam conditions for the changes of irradiation hardening was not detected at 270 °C.

3.2. Swelling behavior under ion irradiations

In a previous study [8,9], swelling behavior of F82H steel was examined at temperatures of 470,

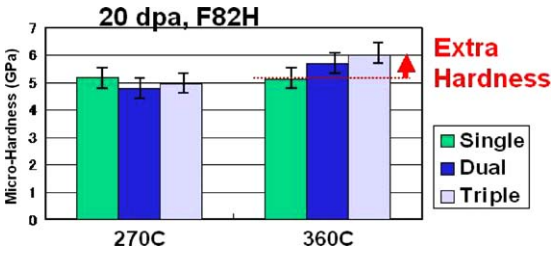

Fig. 5. Changes of hardness of F82H steel irradiated at 270 and 360 °C to 50 dpa.

510 and 600 °C to 50 dpa under dual ion beams of about 15 appm He/dpa and triple ion beams of 15 or 150 appm He/dpa and 50 or 1000 appm He/dpa. These swelling ranged from about 0.1% to 3%, and the swelling was enhanced by the synergistic effect of helium, hydrogen and displacement damage under the triple ion beams.

In present study, swelling behavior is examined at temperatures of 360 and 430 °C to 50 dpa under dual ion beams. Fig. 6(a) and (b) show microstructures of F82H steels formed at 360 and 430 °C to 50 dpa by dual ion beams of Fe and He ions, respectively. The microstructures formed by 360 °C irradiation in F82H steel were only dislocation loops as shown in Fig. 6(a). Many cavities and dislocation loops were formed in F82H irradiated at 430 °C to 50 dpa, and the swelling was about 0.6%. The size distribution of cavities was bi-modal. In Fig. 7, the swelling of F82H irradiated by dual ion beams is given as a function of temperature, and the swelling peak temperature is around 430 °C.

In previous studies of swelling by neutron irradiation [12,15], the effect of helium production on swelling of F82H irradiated at 300 and 400 °C to 51 dpa by neutrons in HFIR (High Flux Isotope Reactor) was examined by using a ^{10}B doping technique. The swelling at 400 °C tended to increase from 0.1% to 1.1% with increasing helium production from about 10 to 330 appm, and the swelling at 300 °C was very low and small cavities with low number density was formed in F82H steel with a helium production of about 330 appm. In the previous swelling study due to helium production in F82H steel, the ratio of helium production to displacement damage was not controlled during irradiation. In the present study, the ratio of helium to displacement damage was controlled during irradiation.

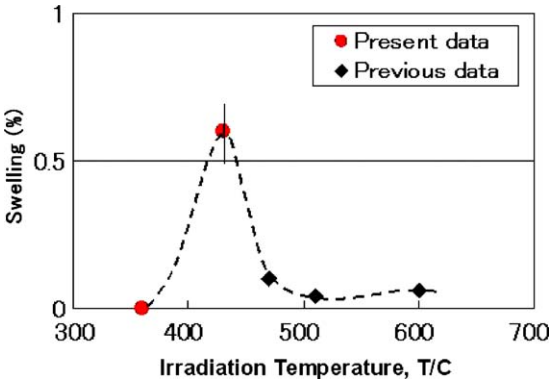

Fig. 7. Dependence of irradiation temperature for swelling of F82H steel irradiated with dual beams to 50 dpa.

3.3. Effect helium on fracture behavior at high temperature by SP test

Fig. 8(a) and (b) show microstructures taken under low and high magnifications, respectively, by a transmission electron microscope for F82H steel implanted to about 84 appm helium and about 0.03 dpa by 50 MeV He^{2+} ions at about 120 °C using an energy degrader of aluminum foils for

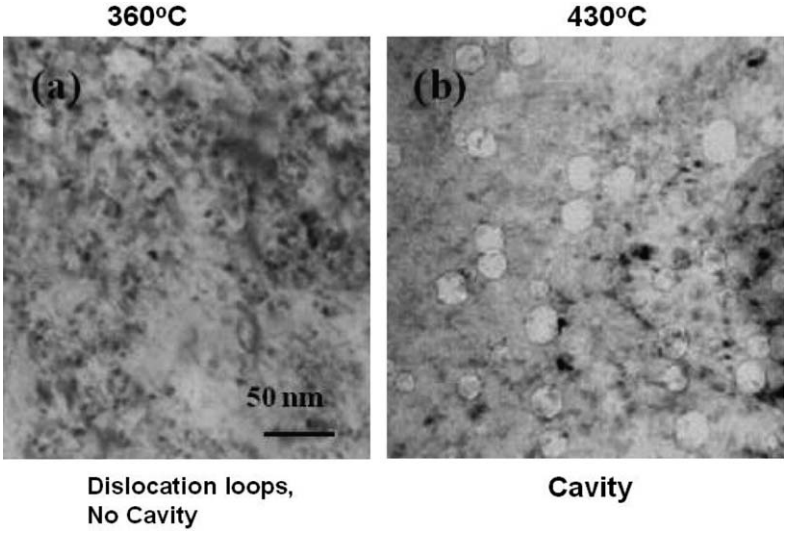

Fig. 6. Microstructures formed in F82H steels irradiated with dual beams at (a) 360 °C and (b) 430 °C to 50 dpa.

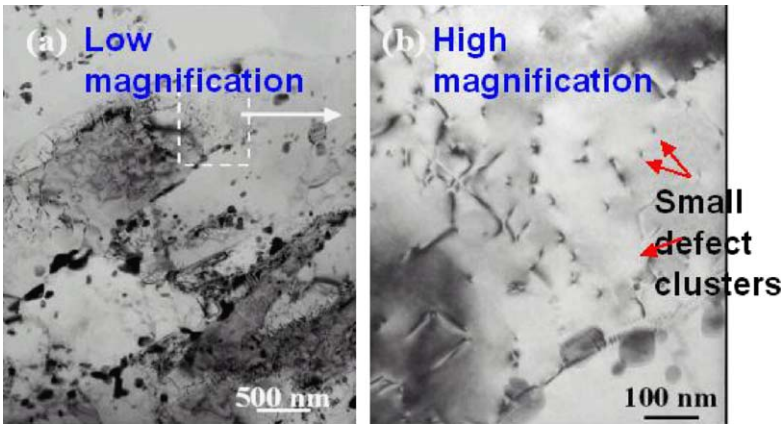

Fig. 8. Microstructures of (a) low and (b) high magnification figures in F82H steel implanted with 50 MeV He^{2+} ions at 120 °C to 0.03 dpa.

helium ions. In the micrographs, dislocations, carbides, lath boundaries and small defect clusters like dislocation loops were observed. The number density of small defect clusters formed by the irradiation was very low. Cavities were not observed in the specimen.

The curves of load–displacement for the SP tests at 600 and 700 °C in F82H steels with and without after the helium implantation were given in Fig. 9. In the specimens implanted with helium, larger stress occurred as seen in Fig. 9(a) and (b), especially in the specimen tested at 600 °C. In the helium-implanted specimens, the elongations were not degraded. After the SP tests, the fracture surfaces were observed by SEM as shown in Figs. 10 and 11. The ductile fracture surfaces were observed in all specimens. No cracking at grain boundaries were observed in all specimens tested at 600 and 700 °C. Small cavity like blisters at the cracked region were formed near outside the surface of the non-helium-implanted specimen tested at 700 °C, however, such cavities were not observed in the helium-implanted specimen tested at 700 °C. The formation of the cavities near the surface after SP test was also observed in only the non-helium-implanted specimen tested at 600 °C.

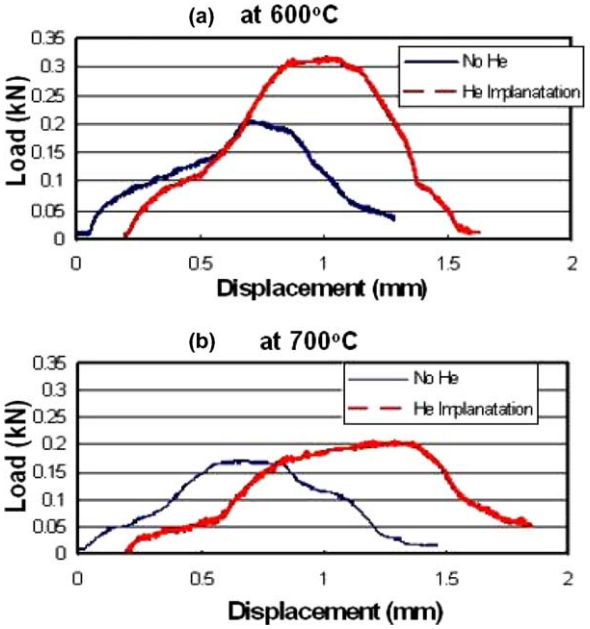

Fig. 9. The curves of load–displacement for the SP tests at 600 and 700 °C in F82H steels with and without after the helium implantation.

3.4. Effect of helium production on fracture toughness of F82H steel

Fig. 12 shows ΔYS due to neutron irradiation in F82H + ^{11}B, F82H + ^{10}B + ^{11}B and F82H + ^{10}B steels irradiated at 300 °C to 2.3 dpa as reported in previous study [3]. The tensile test temperatures were performed at 20, 300 and 400 °C. Small increment of ΔYS due to helium production was observed in F82H + ^{10}B steel with helium production of about 330 appm. Similar results are obtained in the present ion irradiation experiment and the other studies as described in Section 3.1. Therefore, helium production can be affect the microstructural evolution and irradiation hardening.

In this study, the effect of helium production on fracture toughness has been examined. Fig. 13 shows curves of load vs. displacement for fracture

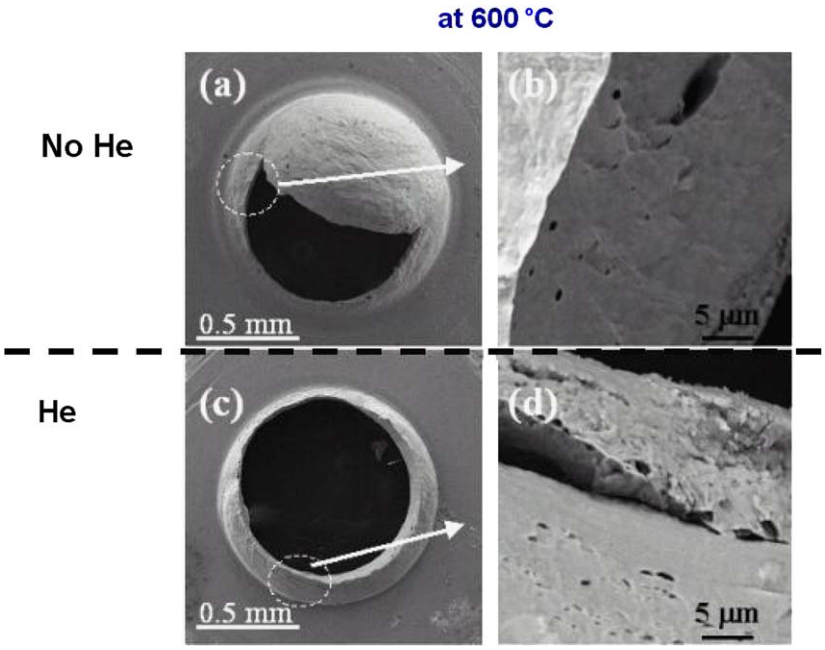

Fig. 10. SEM micrographs of (a) no-helium and (b) helium implanted F82H specimens tested at 600 °C after small punch.

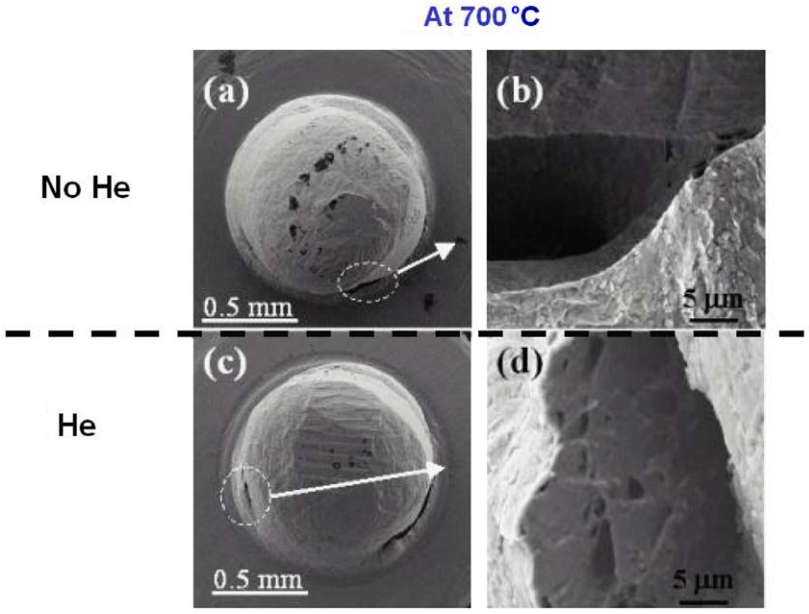

Fig. 11. SEM micrographs of (a) no-helium and (b) helium implanted F82H specimens tested at 700 °C after small punch.

toughness specimens irradiated at 300 °C to 2.3 dpa. The amounts of helium production in F82H + ^{11}B and F82H + ^{10}B steels are about 5 appm and 330 appm, respectively. The maximum loads of the irradiated F82H + ^{11}B and F82H + ^{10}B steels were about 2.5 and 2.9 kN, respectively. As the maximum load was exceeded, the strength of F82H + ^{11}B steel decreased gradually, while that of F82H + ^{10}B steel rapidly decreased and the fracture proceeded to the end of specimen after the displacement of only 2.2 mm. SEM micrographs after the fracture tests at 300 °C are shown in Fig. 14. The surface of

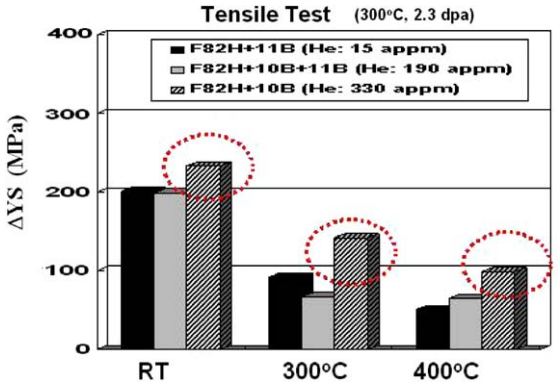

Fig. 12. ΔYS due to neutron irradiation in F82H + ^{11}B, F82H + ^{10}B + ^{11}B and F82H + ^{10}B steels irradiated at 300 °C to 2.3 dpa.

F82H + ^{11}B steel with no helium production was relatively smooth, but the fracture surface of F82H + ^{10}B steel with helium production was very rough. The cause would be related to the occurrence of sub-boundary, such as lath boundaries and packed boundaries, cracking due to helium migration to sub-boundaries. Brittle fracture surfaces of F82H + ^{11}B and F82H + ^{10}B steels were observed at −50 °C and 100 °C, respectively. The difference of temperature was about 140 °C. The fracture surfaces of F82H + ^{11}B and F82H + ^{10}B steel in the brittle temperature regions were observed by a SEM as given in Fig. 15. The surface of F82H + ^{11}B steel with no helium production was cleavage, but F82H + ^{10}B steel with helium production was somewhat rough on the fracture surface.

3.5. Design window of martensitic steels for irradiation environment systems

Post testing at high temperature, 600 and 700 °C, following low temperature helium implantation shows enhancement of hardening without degradation due to helium. Similar result was reported by H. Schroeder [36]. In martensitic steel, the decrease of creep strength at higher temperature is one of its draw backs negative properties. The design window of safety zone map for operation in fusion nuclear reactor using a water coolant system or other

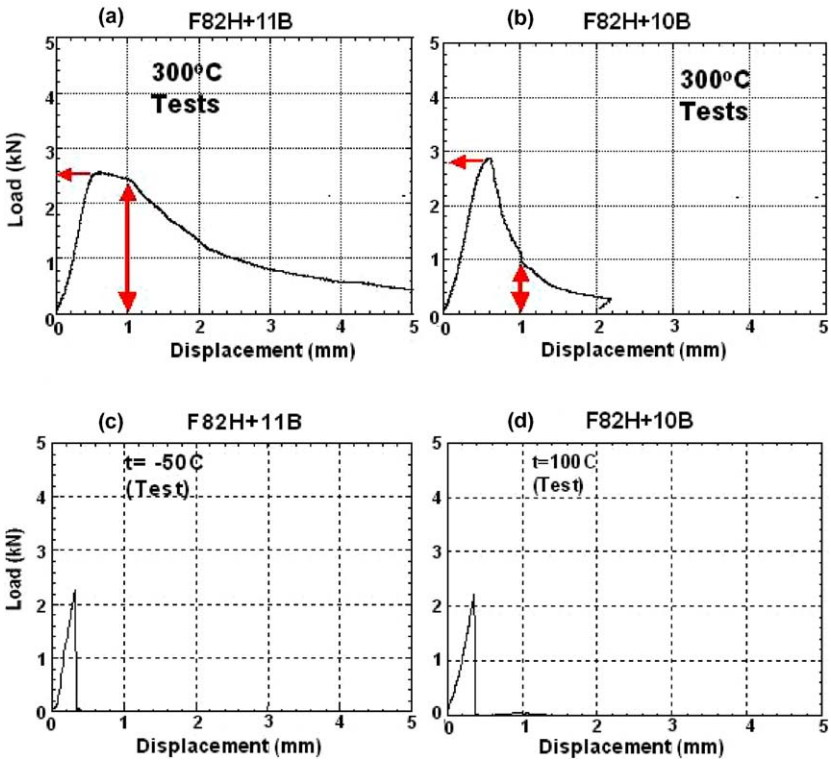

Fig. 13. Curves of load and displacement of 0.18DCT fracture toughness specimens irradiated at 300 °C to 2.3 dpa. (a) F82H + ^{11}B tested at 300 °C, (b) F82H + ^{10}B tested at 300 °C, (c) F82H + ^{11}B tested at −50 °C, and (d) F82H + ^{10}B tested at 100 °C.

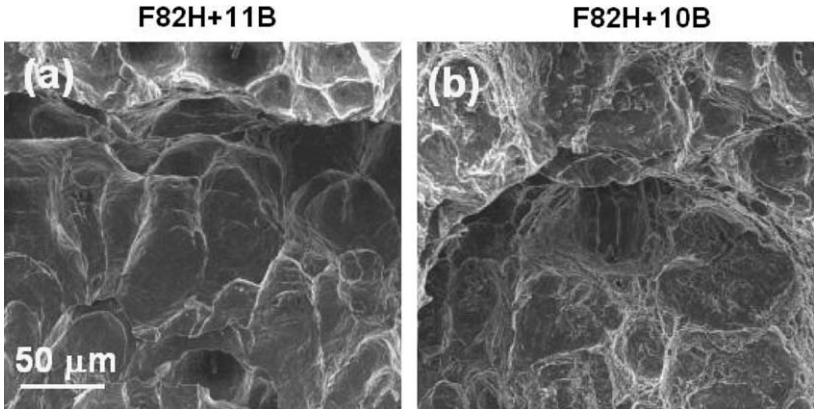

Fig. 14. SEM micrographs of F82H + ^{11}B and F82H + ^{10}B steels irradiated at 300 °C to 2.3 dpa after the fracture testing at 300 °C.

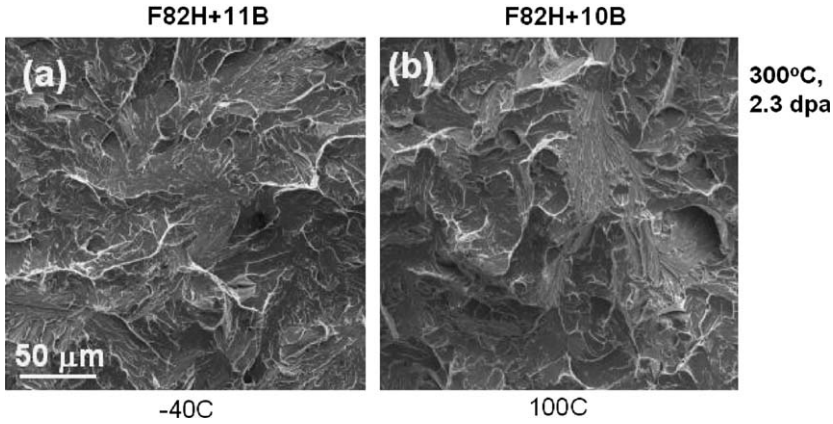

Fig. 15. SEM micrographs of F82H + ^{11}B and F82H + ^{10}B steels irradiated at 300 °C to 2.3 dpa after the fracture testing at lower temperature.

systems, based on data and knowledge about properties of reduced-activation ferritic/martensitic steels, was restricted at higher temperature by loss of creep strength or softening during irradiation [1]. However, the strength at higher temperature in the helium content specimen is larger than that in the non-content helium specimen, therefore, the safety zone at higher temperature may be modified by the suppression of deformation due to helium production.

The effects of helium production on swelling and fracture toughness as shown in Sections 3.2 and 3.4 can be also affected on the design window of martensitic steels for irradiation environment systems, and the enhancement of swelling due to gas atoms and the shift of DBTT due to helium atoms are negative effects. We would have to take care of these effects to operate these systems.

4. Conclusion

Effects of gas atoms on microstructures and mechanical properties of F82H steel irradiated by ions were examined as described below:

(1) The hardness of F82H was increased by triple beams, dual beams and single beam at 270 °C to 20 dpa and 360 °C to 50 dpa, and the increment of hardness by irradiation at 360 °C was larger than that at 270 °C. The increment of hardness due to triple, dual and single beams depended on the irradiation temperatures.
(2) The peak temperature of swelling induced by dual ion beams to 50 dpa was about 430 °C at temperatures from 360 to 600 °C and the value of swelling was about 0.6%.

(3) The strength of F82H-std implanted with helium at 120 °C resulted in increased strength at 600 and 700 °C of SP test temperatures, and no degradation in ductility was observed.
(4) As crack extends in ductile temperature region, strengths of F82H with helium production become lower than that with no helium production. The cause is related to sub-boundary crack.
(5) Brittle fracture surfaces of F82H + ^{11}B and F82H + ^{10}B steels were observed at −50 °C and 100 °C, respectively. The difference of temperature was about 140 °C.
(6) The design window of safety zone of RAF steels for operation of nuclear environment systems may be modified by the suppression of deformation due to helium production at higher temperature, the enhancement of swelling due to gas atoms and the shift of DBTT due to helium.

Acknowledgements

The authors would like to thank the members of TIARA facility of JAEA for their operations of the accelerators and managements. It is also a pleasure to acknowledge the support of the members of the Oarai and Tokai Hot Laboratory of JAEA.

References

[1] M. Kawai, J. Nucl. Mater. 318 (2003) 371.
[2] Hishinuma, A. Kohyama, R.L. Klueh, D.S. Gelles, W. Dietz, K. Ehrlich, J. Nucl. Mater. 258–263 (1998) 193.
[3] E. Wakai, S. Jitsukawa, H. Tomita, K. Furuya, M. Sato, K. Oka, T. Tanaka, F. Takada, T. Yamamoto, Y. Kato, Y. Tayama, K. Shiba, S. Ohnuki, J. Nucl. Mater. 343 (2005) 285.
[4] M. Rieth, B. Dafferner, H.D. Rouhrig, J. Nucl. Mater. 258–263 (1998) 1147.
[5] D.S. Gelles, J. Nucl. Mater. 283–287 (2000) 838.
[6] E.I. Materna-Morris, M. Rieth, K. Ehrich, Effects of Radiation on Materials, STP1366, p. 597.
[7] K. Shiba, I. Ioka, J.P. Robertson, M. Suzuki, A. Hishinuma, Euromat 96 (1996) 265.
[8] E. Wakai, K. Kikuchi, S. Yamamoto, T. Aruga, M. Ando, H. Tanigawa, T. Taguchi, T. Sawai, K. Oka, S. Ohnuki, J. Nucl. Mater. 318 (2003) 267.
[9] E. Wakai, T. Sawai, K. Furuya, A. Naito, T. Aruga, K. Kikuchi, S. Yamashita, S. Ohnuki, S. Yamamoto, H. Naramoto, S. Jitsukawa, J. Nucl. Mater. 307–311 (2002) 278.
[10] T. Sawai, E. Wakai, K. Tomita, A. Naito, S. Jitsukawa, J. Nucl. Mater. 307–311 (2002) 312.
[11] T. Tanaka, K. Oka, S. Ohnuki, S. Yamashita, T. Suda, S. Watanabe, E. Wakai, J. Nucl. Mater. 329–333 (2004) 294.
[12] E. Wakai, N. Hashimoto, Y. Miwa, J.P. Robertson, R.L. Klueh, K. Shiba, S. Jitsukawa, J. Nucl. Mater. 283–287 (2000) 799.
[13] Y. Miwa, E. Wakai, K. Shiba, N. Hashimoto, J.P. Robertson, A.F. Rowcliffe, A. Hishinuma, J. Nucl. Mater. 283–287 (2000) 334.
[14] T. Morimura, A. Kimura, H. Matsui, J. Nucl. Mater. 239 (1996) 118.
[15] E. Wakai, Y. Miwa, N. Hashimoto, J.P. Robertson, R.L. Klueh, K. Shiba, K. Abiko, S. Furuno, S. Jitsukawa, J. Nucl. Mater. 307–311 (2002) 203.
[16] M. Ando, E. Wakai, H. Tanigawa, T. Sawai, K. Furuya, S. Jitsukawa, H. Takeuchi, K. Oka, S. Ohnuki, A. Koyama, J. Nucl. Mater. 329–333 (2004) 1137.
[17] Y. Katoh, H. Taniga wa, T. Muroga, T. Iwai, A. Kohyama, J. Nucl. Mater. 271&272 (1999) 115.
[18] M. Ando, H. Tanigawa, S. Jitsukawa, T. Sawai, Y. Katoh, A. Kohyama, K. Nakamura, H. Takeuchi, J. Nucl. Mater. 307–311 (2002) 260.
[19] J. Henry, X. Averty, Y. Dai, P. Lamagnere, J.P. Pizzanelli, J.J. Espinas, P. Wident, J. Nucl. Mater. 318 (2003) 215.
[20] N. Hashimoto, J.D. Hunn, T.S. Byun, L.K. Mansur, J. Nucl. Mater. 318 (2003) 300.
[21] K. Farrel, T.S. Byun, J. Nucl. Mater. 318 (2003) 274.
[22] E. Wakai, T. Taguchi, T. Yamamoto, H. Tomita, F. Takada, S. Jitsukawa, Mater. Trans., JIM 46 (2005) 481.
[23] E. Wakai, S. Matsukawa, T. Yamamoto, Y. Kato, F. Takada, M. Sugimoto, S. Jitsukawa, Mater. Trans. 45-8 (2004) 2641.
[24] Y. Dai, X.J. Jia, K. Farrel, J. Nucl. Mater. 318 (2003) 192.
[25] S.A. Maloy, M.R. James, W.R. Johnson, T.S. Byun, K. Farrel, M.B. Toloczko, J. Nucl. Mater. 318 (2003) 283.
[26] R. Kasada, A. Kimura, H. Matsui, M. Narui, J. Nucl. Mater. 258–263 (1998) 1199.
[27] R.L. Klueh, M.A. Sokolov, K. Shiba, Y. Miwa, J.P. Robertson, J. Nucl. Mater. 283–287 (2000) 478.
[28] T. Sawai, M. Ando, E. Wakai, K. Shiba, S. Jitsukawa, Fusion Sci. Technol. 44-1 (2003) 201.
[29] A. Kimura, T. Morimura, R. Kasada, H. Matsui, A. Hasegawa, K. Abe, Effects of Radiation on Materials, in: Proc. of 19th Symp. p. 626.
[30] N. Yamamoto, J. Nagakawa, K. Shiba, J. Nucl. Mater. 400 (2000) 283.
[31] N. Yamamoto, Y. Murase, J. Nagakawa, K. Shiba, J. Nucl. Mater. 217 (2002) 307.
[32] P. Jung, J. Henry, J. Chen, J.-C. Brachet, J. Nucl. Mater. 318 (2003) 241.
[33] J. Henry, M.-H. Mahton, P. Jung, J. Nucl. Mater. 318 (2003) 249.
[34] W.D. Oliver, G.M. Pharr, J. Mater. Res. 7 (1992) 1564.
[35] Y. Miwa et al., JAERI – Rev. 97-015 (1997) 108.
[36] H. Schroeder, H. Ullmaier, J. Nucl. Mater. 118 (1991) 179.